Journal of Physiology (1990), **427**, *pp.* 657–680
With 12 figures
Printed in Great Britain

CALCIUM CURRENTS IN ISOLATED RABBIT CORONARY ARTERIAL SMOOTH MUSCLE MYOCYTES

BY J. J. MATSUDA, K. A. VOLK AND E. F. SHIBATA*

From the Department of Physiology and Biophysics, University of Iowa, College of Medicine, Iowa City, IA 52242, USA

(*Received 13 July 1989*)

SUMMARY

1. Calcium inward currents were recorded from relaxed enzymatically isolated smooth muscle cells from the rabbit epicardial left descending coronary artery using a single-pipette voltage-clamp technique. Outward K^+ currents were blocked with CsCl–tetraethylammonium-filled pipette solutions.

2. Relaxed coronary smooth muscle cells had a maximum diameter of $8{\cdot}6 \pm 0{\cdot}6$ μm and a cell length of $96{\cdot}7 \pm 3{\cdot}3$ μm when bathed in 2·5 mM $[Ca^{2+}]_o$. The average resting membrane potential at room temperature was -32 ± 10 mV. The mean cell capacitance was $18{\cdot}5 \pm 1{\cdot}7$ pF and the input resistance was $3{\cdot}79 \pm 0{\cdot}58$ GΩ.

3. Depolarizing voltage-clamp steps from a holding potential of −80 mV elicited a single time- and voltage-dependent inward current which was dependent upon extracellular $[Ca^{2+}]$. In 2·5 mM $[Ca^{2+}]_o$, the inward current was activated at a potential of −40 mV and peaked at +10 mV. This current was inhibited by 0·5 mM-$CdCl_2$ and 1 μM-nifedipine and was enhanced with 1 μM-Bay K 8644. No detectable low-threshold, rapidly inactivating T-type calcium current was observed.

4. The apparent reversal potential of this inward current in 2·5 mM $[Ca^{2+}]_o$ was +70 mV and shifted by 33·0 mV per tenfold increase in $[Ca^{2+}]_o$. This channel was also more permeable to barium and strontium ions than to calcium ions.

5. Single calcium channel recordings with 110 mM-Ba^{2+} as the charge carrier revealed a mean slope conductance of $20{\cdot}7 \pm 0{\cdot}8$ pS.

6. This calcium current (I_{Ca}) exhibited a strong voltage-dependent inactivation process. However, the steady-state inactivation curve (f_∞) displayed a slight non-monotonic, U-shaped dependence upon membrane potential. The potential at which half of the channels were inactivated was −27·9 mV with a slope factor of 6·9 mV. The steady-state activation curve (d_∞) was also well-described by a Boltzmann distribution with a half-activation potential at −4·4 mV and a slope factor of −6·3 mV. I_{Ca} was fully activated at approximately +20 mV.

7. The rate of inactivation was dependent upon the species of ion carrying the current. Both Sr^{2+} and Ba^{2+} decreased the rate as well as the degree of inactivation. The τ_f (fitted time constant of inactivation) curve displayed a U-shaped relationship in 2·5 mM $[Ca^{2+}]_o$. The reactivation process was voltage dependent and could be described by a single exponential.

* To whom all correspondence and reprint requests should be sent.

MS 7832

8. The current amplitude and the inactivation kinetics were temperature dependent. The Q_{10} for peak current amplitude was 1·57.

9. Bath application of 0·2 μM-ACh increased I_{Ca} by approximately 40% of control in eight of thirteen cells. This enhanced ACh effect was blocked by 1 μM-atropine in all eight cases.

INTRODUCTION

The large epicardial coronary arteries play an important role in regulating myocardial blood flow (Chilean, Eastham & Marcus, 1986) and are the site of the localized spasm seen in patients with variant angina pectoris (Shepherd & Vanhoutte, 1986). Although many physiological studies have been done on coronary arteries (for review see Feigl, 1983), very little work has been published on the voltage-dependent calcium channels of isolated coronary artery smooth muscle cells (Klockner & Isenberg, 1985*a*, *b*). Electrophysiological measurements using standard microelectrode techniques showed that smooth muscle cells from the dog coronary artery do not normally exhibit action potentials when electrically stimulated (Harder, Belardinelli, Sperelakis, Rubio & Berne, 1979; Mekata, 1980). However, when outward potassium currents were inhibited with the addition of tetraethylammonium (TEA), electrical stimulation elicited overshooting action potentials which were inhibited with calcium channel blockers.

Two types of calcium currents have been identified in smooth muscle cells from numerous vascular tissues (for reviews see Aaronson, Bolton, Lang & MacKenzie, 1988; Bean, 1989). In high-barium solutions one type of calcium current, the transient (T-type) or low-threshold (I_{low}) current is typically present at holding potentials negative to −30 mV, activates near −40 mV, inactivates completely within 100 ms and is insensitive to dihydropyridines. The long-lasting (L-type) or high-threshold calcium current (I_{high}) can be elicited from a holding potential of −30 mV, activates near −20 mV, does not completely inactivate during test pulses of 200 ms or more and is sensitive to dihydropyridines. However, a clear distinction between the low-threshold, T-type calcium current and the high-threshold, L-type calcium current in rabbit ear artery smooth muscle cells remains unclear (Aaronson *et al.* 1988). While some of their results are consistent with the above classification scheme, they show calcium currents elicited from potentials negative to −50 mV which activate between −60 and −40 mV and which do not completely inactivate during a 500 ms depolarization. A similar type of calcium current was also observed in segments of proximal rat middle cerebral arteriolar tissue (Hirst, Silverberg & van Helden, 1986). A recent study suggests that there are populations of cells which are rich in one channel type over the other; the 'healthier' cells having a greater population of L-type channels (Benham, Hess & Tsien, 1987).

Recent studies also show that vascular smooth muscle calcium channels can be modulated by adrenergic agonists (Benham & Tsien, 1988; Droogmans, Declerck & Casteels, 1987; Nelson, Standen, Brayden & Worley, 1988) although the effects of cholinergic agonists have not been investigated. The effects of acetylcholine on coronary artery are species dependent (for review see Kalsner, 1989). Acetylcholine constricts the rabbit coronary artery strip and this effect is inhibited by atropine (De La Lande, Harvey & Holt, 1974). It is therefore of particular interest to determine

the manner in which calcium currents in rabbit coronary arteries respond to acetylcholine.

The mechanism by which vascular smooth muscle calcium currents inactivate has not been fully investigated. It is generally accepted that inactivation is voltage dependent in smooth muscle cells (Klockner & Isenberg, 1985*c*; Yatani, Seidel, Allen & Brown, 1987). There is also evidence for calcium-dependent inactivation in guinea-pig taenia caeci smooth muscle cells (Ganitkevich, Shuba & Smirnov, 1986, 1987).

We report here a detailed study of calcium currents from enzymatically dispersed vascular smooth muscle cells from the rabbit left anterior descending coronary artery. The two major findings presented in this paper are: (1) there appears to be only one type of calcium current (L-type), and (2) the inactivation process can be described by a both Ca^{2+}- and voltage-dependent mechanism.

METHODS

Solutions and drugs

Zero Ca^{2+} solution contained modified Tyrode solution without the addition of calcium. Cell suspension storage media contained zero Ca^{2+} solution to which bovine serum albumin (0·1 %) and taurine (20 mM) were added. The solutions were made with drugs and chemicals obtained from Sigma Chemical Co. (St Louis, MO, USA). Nifedipine and Bay K 8644 (Calbiochem Corp., San Diego, CA, USA) were dissolved in ethanol to a 1 mM stock solution and serially diluted in superfusion solution. The solvent concentration was less than 0·01 % and had no detectable effect on the calcium current.

Single cell isolation procedure

New Zealand White rabbits (1·5–2·0 kg) were anaesthetized with an intramuscular injection of a mixture of ketamine HCl (22 mg/ml), xylazine (5·5 mg/ml) and acepromazine (0·5 mg/ml) at a concentration of 0·6 ml/kg. Their hearts were quickly removed and mounted on a modified Lagendorff apparatus for perfusion (25 ml/min) of the coronary circulation. After an initial 5 min of perfusion at 37 °C with modified Tyrode solution, zero Ca^{2+} solution was perfused for an additional 5 min. This was followed by a 10 min perfusion of zero Ca^{2+} solution containing 0·1 mg/ml collagenase (Sigma type I) and 0·03 mg/ml trypsin inhibitor (Sigma type II-S). The coronary circulation was then perfused with enzyme-free zero Ca^{2+} Tyrode solution for 5 min. The left anterior descending coronary artery (proximal 2 cm, 1–2 mm outside diameter) was carefully removed with a portion of the myocardium attached and pinned to the bottom of a silicone elastomer (Sylgard 184; Dow Corning Co. Midland, MI, USA) filled dissection dish. The adhering ventricular myocardium was then carefully removed so as not to cause overstretching of the vessel. The coronary artery was slit longitudinally and placed into a small vial containing zero Ca^{2+} solution with 1 mg/ml collagenase (Sigma type I), 0·4 mg/ml trypsin inhibitor (Sigma type II-S), and 0·4 mg/ml elastase (Sigma type IV). The tissue was gently stirred in a temperature regulated bath at 35 °C for approximately 30 min. The supernatant was discarded and cell suspension storage media was added. The tissue was then triturated with a fire-polished Pasteur pipette (tip diameter approximately 2 mm). Trituration of the tissue usually resulted in a consistent relatively high yield (60 %) of elongated single coronary smooth muscle cells.

Experimental procedure

The recording chamber consisted of a 13 × 1·5 mm lucite ring cemented to a standard microscope glass slide with Sylgard 184. This was mounted on a moveable stage mounted on a Nikon Diaphot (TMD) or a Nikon TMS inverted microscope. The volume of the recording chamber was 0·15–0·2 ml. An aliquot of single coronary arterial smooth muscle cells in suspension was added in the chamber and allowed to settle to the bottom for 10–20 min. Solutions were then superfused through the chamber by gravity at a rate of 0·2–0·4 ml/min. All experiments were performed at

room temperature (21–23 °C) except where temperature dependent experiments were done. In these experiments, temperature regulation was achieved by placing the chamber slide on a resistive heating element which was regulated by a battery-powered feedback controller (Brook Industries, Lake Villa, IL, USA). A miniature thermistor was placed near the cell to monitor the bath temperature. This unit provided a stable temperature (±0·1 °C) and a change of 10 °C could be achieved within approximately 3 min.

TABLE 1. Composition of solutions (mM)

Chemicals	Modified Tyrode solution	Isotonic barium	Normal pipette	CsCl–TEA	Single-channel	
					Pipette	Bath
NaCl	140	0	0	0	0	0
KCl	4·5	0	140	0	0	0
CsCl	0	0	0	120	0	0
Potassium aspartate	0	0	0	0	0	140
$CaCl_2$	2·5	0	0·552	0	0	0
$MgCl_2$	1	0	1	1	0	1
$BaCl_2$	0	110	0	0	110	0
HEPES	10	10	10	10	10	5
Glucose	5·5	10	0	0	10	20
EGTA	0	0	0	5	0	5
Na_2ATP	0	0	4	5	0	0
TEA-Cl	0	0	0	22	20	20
4-AP	0	0	0	0	2	2
pH	7·35	7·35	7·2	7·2	7·35	7·35
Titrant (1 M)	NaOH	CsOH	KOH	CsOH	KOH	KOH

Both whole-cell and cell-attached patch-clamp recordings were similar to that originally described by Hamill, Marty, Neher, Sakmann & Sigworth (1981). Pipettes were fabricated from borosilicate glass capillaries (1·8 mm o.d.; Kimax-51) and pulled on a vertical pipette puller (PP-83; Narishige Scientific Instrument Laboratories, Tokyo, Japan). Pipette tips were coated with a thick layer of Sylgard 184 to within 50–100 μm from their tips with a 30 gauge needle and fire-polished on a home-made microforge mounted on a Nikon Labophot microscope. The pipette tip was viewed at 600× magnification using an extra-long working-distance objective. The pipettes used for whole-cell voltage-clamp recordings had resistances of 2–4 MΩ when filled with CsCl–TEA pipette solution. The pipette tip was positioned near the nuclear region of the coronary smooth muscle cell using a hydraulic micro-manipulator (Model MO-102; Narishige Scientific Instruments, Tokyo, Japan). A membrane–pipette seal was established by gently touching the cell and applying suction to the pipette interior. The resistance of the seal ranged from 20–90 GΩ. For whole-cell recordings, the sealed membrane patch was ruptured after waiting 1–2 min before an additional suction was applied.

Membrane currents were acquired using an Axopatch-1B patch-clamp amplifier (Axon Instruments, Inc., Burlingame, CA, USA) and filtered with a 4-pole low-pass Bessel filter having a bandwidth (−3 dB) of 1 kHz. Current signals were digitized on-line at a sampling frequency of 4 kHz. Voltage-clamp command potentials were generated using the pCLAMP software (Axon Inst., Inc., Burlingame, CA, USA).

Series resistance (R_s) and cell membrane capacitance (C_m) were determined from small 10 mV voltage-clamp steps from a holding potential V_h of −80 mV (Johnson & Lieberman, 1971). In our determination of R_s and C_m, the current transient was filtered at 20 kHz and digitized at a rate of 24 μs/sample. R_s was determined by dividing the 10 mV voltage step by the zero-time initial amplitude of the uncompensated current transients; $R_s = \Delta V/I(0)$. Time constants and initial amplitudes were determined by the DISCRETE curve-fitting program (see below) and were best-fitted to one exponential in more than 90% of all cases ($n = 22$). The R_s from twenty-two measurements was calculated to be 6·37 ± 0·95 MΩ (mean ± S.E.M.). The R_s was consistently found

to be approximately 2–3 times the initial pipette resistance, possibly due to partial occlusion of the pipette tip by cytoplasmic material (Marty & Neher, 1983). Series resistance could be typically reduced by 70–80% after adjusting the internal compensation circuitry of patch-clamp amplifier to give the fastest capacitance transient before oscillation. C_m was determined by dividing the fitted time constant (τ_f) by the calculated R_s value ($C_m = \tau_f/R_s$). Capacitance and 'leak' currents were corrected by applying 0·3 mM-$CdCl_2$ to block the calcium currents. The cadmium-blocked current record was then subtracted from the current traces at each potential. The internal perfusion technique described by Neher & Eckert (1987) was used in some experiments (see Figs 1 and 7) without modification.

Single-channel experiments were performed in the cell-attached mode. This was necessary because channel activity gradually disappeared if the patch was excised. Cell-attached single-channel currents were recorded using the Axopatch-1B patch-clamp amplifier with a gain of 0·1 V/pA. The current output was filtered at 1 kHz with a 4-pole Bessel filter and digitized at 6·67 kHz. Fabrication of patch pipettes were similar to that used in whole-cell current recordings. Patch pipettes filled with single-channel pipette solution (110 mM-$BaCl_2$) had resistances of 1–2 MΩ. Single-channel currents were evoked by depolarizing the membrane patch from a holding potential at −80 mV for 150–250 ms. The bath solution contained 140 mM-potassium aspartate to 'zero' the membrane potential. To verify that the high-potassium bath solution was effectively 'zeroing' the membrane potential of the cell, a patch was occasionally excised at the end of an experiment and the single-channel amplitudes were compared to cell-attached amplitudes at restricted potentials. There were no significant differences between amplitudes measured before and after patch excision. Capacitative and 'leak' currents were corrected for by averaging the traces where no channel activity occurred and subtracting the averaged trace from each record.

Data recording and analysis

Membrane current and voltage were monitored on a storage oscilloscope (V-134; Hitachi Denshi Ltd, Japan) and simultaneously stored on tape using a two-channel PCM recorder adapter (PCM-1, analog-to-digital converter, 22 kHz/channel; Medical Systems Co., Greenville, NY, USA) and a video recorder (Sony SL-HF650, Super Beta). Membrane current data were digitized on-line or at a later time using a 12-bit resolution A/D converter (40 kHz, Labmaster TM40; Scientific Solutions, Inc., Solon, OH, USA) and stored on the hard disc of an IBM PC/AT computer. Digitized data were transmitted from the IBM-AT to a DEC VAX 11/780 computer for curve fitting. Whole-cell and single-channel current data were analysed on the IBM-AT using the pCLAMP software (Axon Instruments, Inc., Burlingame, CA, USA).

Curve fitting

Current transients were fitted to sums of exponentials (from one to four) using a FORTRAN IV version of the DISCRETE program developed by Provencher (1976). This analysis program is based on the Fourier convolution theorem. It determines the number of exponential terms from discrete spectra which best describes the time course of a selected data segment and computes the initial amplitude and time constant of each exponential term. When the program finds more than one possible fit, the solution with the larger number of components is tested for the probability of being a better fit to the data by using a Fisher's F distribution. This statistical procedure defines the distribution as the sampling distribution of the ratio of two independent χ^2 random variables, each divided by its respective degrees of freedom. In addition to the F distribution, the standard error and the standard deviation of the fit also determine the goodness of fit. Conclusions regarding the number of components in a specific process were based on a number of cells recorded under similar conditions and all fits were inspected visually. Difficulties with this fitting procedure can arise if (1) the time constants are orders of magnitude larger than the length of the data segment or (2) two exponential components have almost identical time constants. We feel that the Provencher method provides an objective means for determining the number of exponential components in data consisting of a sum of exponentials.

RESULTS

General properties of single coronary myocytes

After the enzymatic isolation procedure, approximately 60% of the cells were relaxed and had an elongated appearance in 2·5 mM $[Ca^{2+}]_o$. The remaining cells were either partially or fully contracted with a shortened or rounded appearance. At room temperature, relaxed single coronary artery myocytes had an average resting potential of -32 ± 10 mV ($n = 13$) in 2·5 mM $[Ca^{2+}]_o$ and normal pipette solution. These calcium-tolerant cells had dimensions of $8·6 \pm 0·6$ μm ($n = 85$) in maximum diameter and $96·7 \pm 3·3$ μm (mean ± S.E.M.) in length with tapered ends. To determine the viability of the single cells, we tested whether the relaxed cells were responsive to high-K^+ solutions and autonomic transmitters. Brief application of 70 mM-KCl or 0·1 mM-ACh caused the cells to reversibly contract.

Passive properties of isolated coronary artery smooth muscle cells

The cell capacitance measured in twenty-two cells using the voltage-clamp method (see Methods: Experimental procedure) was $18·5 \pm 1·7$ pF (mean ± S.E.M.). Assuming a specific capacitance of 1 μF/cm^2, the calculated cell surface area was $1·85 \pm 10^3$ μm^2. The input resistance (R_{in}) was measured using 10 mV depolarizing and hyperpolarizing voltage-clamp pulses from a holding potential of -80 mV. In this range of potentials, no time-dependent current was elicited. The resulting change in current was therefore used to calculate R_{in}. The average R_{in} was $3·79 \pm 0·58$ GΩ (mean ± S.E.M., $n = 22$). The specific membrane resistance of 70·1 kΩ cm^2 was calculated using the average surface area of $1·85 \times 10^3$ μm^2.

Since the cells were elongated, the validity of the implicit space clamp assumption was assessed from the following calculation. Assuming a single coronary artery smooth muscle cell to be a linear finite cable terminated by an infinite resistance (open circuit) at both ends (Hume & Giles, 1981), the equation of the steady-state response of a short cable was used (Weidmann, 1952; Jack, Noble & Tsien, 1975). With a cell length (L) of 0·0097 cm, and an intracellular resistance (r_i) of $1·6–2·4 \times 10^9$ Ω cm (Bolton, Lang, Takewaki & Benham, 1985), the space constant was calculated to be 0·12–0·15 cm or approximately 13 times the length of a single cell under conditions of no active conductances ($R_{in} = 3·8$ GΩ). An instantaneous current–voltage experiment was performed in a restricted range of potentials (-40 to $+30$ mV) on a cell that had a large peak calcium current (130 pA), and a maximal conductance of 4·2 nS was determined. This resulted in a space constant within the range of 0·030–0·038 cm which is still three to four times the cell length.

Identification of a calcium current (I_{Ca}) in coronary artery cells

Representative records illustrating the size and time course of the whole-cell currents in 2·5 mM $[Ca^{2+}]_o$ are shown in Fig. 1. The superimposed current traces were elicited with 200 ms depolarizing voltage-clamp pulses from a holding potential of -80 mV to a test potential of $+10$ mV. Using normal pipette solutions with a pCa of 7 (upper trace), a large voltage-dependent outward current was elicited which masked any net inward current. This large outward current was sensitive to changes in internal concentrations of EGTA and extracellular $[Ca^{2+}]$ suggesting that the

major component of this outward current was modulated by internal calcium. When the internal dialysis solution was switched from the normal potassium-containing solution to that containing CsCl–TEA with a pCa > 9 (lower trace), a net inward current was revealed. Hyperpolarizing steps from −80 to −120 mV with a

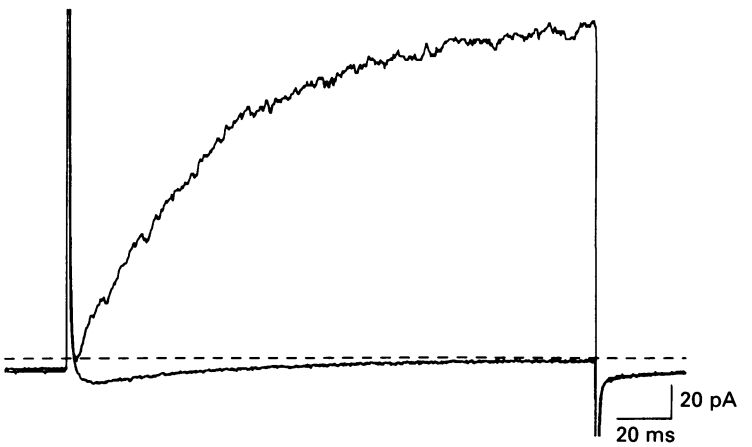

Fig. 1. Block of the outward current using the CsCl–TEA pipette solution. Upper trace: whole-cell current elicited by a 200 ms depolarizing pulse to 10 mV from V_h (holding potential) = −80 mV using the normal pipette solution. Lower trace: current from the same cell using an identical pulse protocol 2 min after internal perfusion of CsCl–TEA solution into the pipette. The dashed line in this and all subsequent current traces indicates the zero current level.

subsequent internal dialysis of CsCl or bath application of 1 mM-$BaCl_2$ in 4·5 mM $[K^+]_o$ (150 mM $[K^+]_i$) produced no measurable current changes indicating the absence of an inwardly rectifying voltage-dependent and time-independent potassium current (I_{K1}). Depolarizing voltage-clamp steps in the range of −70 to +90 mV from a holding potential of −80 mV were used to elicit inward currents. We could only activate an inward current at potential levels positive to −40 mV. This inward current was not altered by high concentrations of tetrodotoxin (TTX, 40 μM), suggesting that smooth muscle cells from the rabbit coronary artery do not contain a TTX-sensitive sodium current.

Ion transfer characteristics of I_{Ca}

The inward current was further characterized by studying its voltage dependence and its $CdCl_2$ sensitivity with the CsCl–TEA pipette solution. Figure 2*A* shows a current–voltage (*I–V*) relationship from a representative cell before (○) and after (●) bath application of 0·5 mM-$CdCl_2$. Cadmium inhibited the inward current throughout the voltage range allowing the $CdCl_2$-sensitive component of the net current to be isolated by subtracting the $CdCl_2$-insensitive current from the net current. Figure 2*B* shows current traces from the same cell after digital subtraction of the $CdCl_2$-insensitive current. The mean *I–V* relationship of the $CdCl_2$-sensitive current from sixteen cells is shown in Fig 2*C* (mean ± S.E.M.). From a holding potential of −80 mV, $CdCl_2$-sensitive currents were elicited using 200 ms depolarizing

voltage-clamp steps from −70 to +90 mV. The mean data shows that an inward current: (i) had a threshold of activation at −40 to −30 mV, (ii) peaked at +10 mV with an average peak amplitude of 45 pA and (iii) had an apparent reversal potential at +70 mV in 2·5 mM $[Ca^{2+}]_o$. The amplitude of the inward current at the peak of the

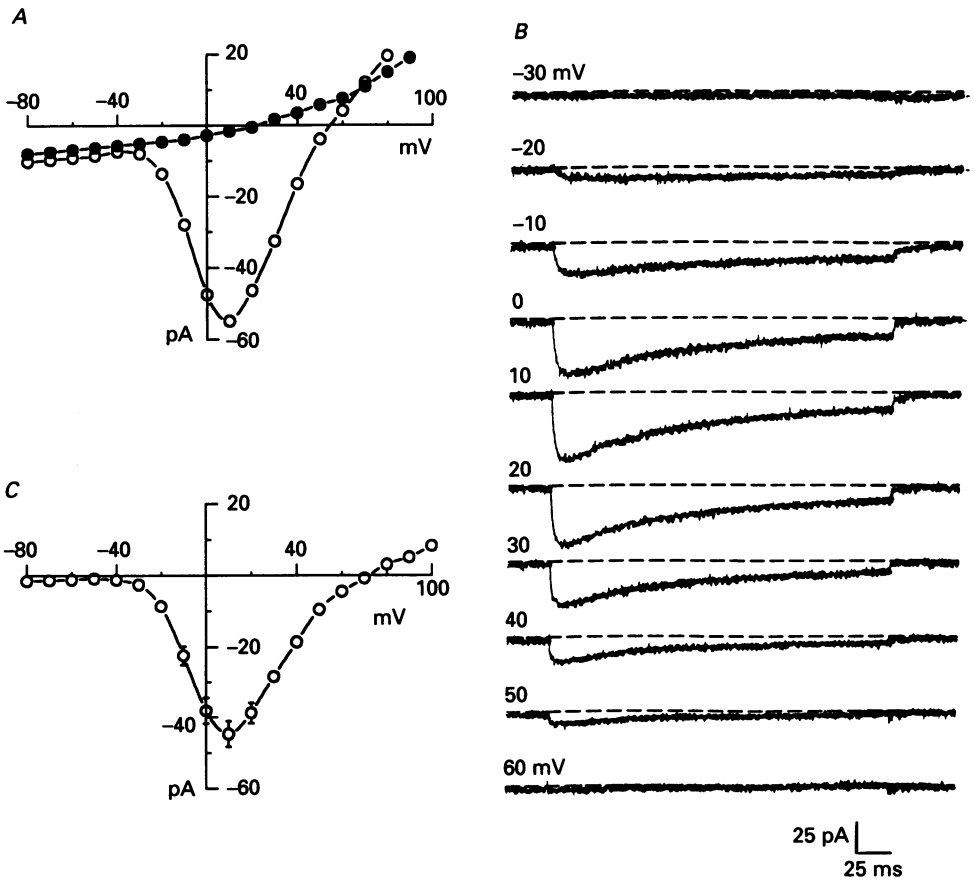

Fig. 2. Voltage dependence of I_{Ca} in 2·2 mM $[Ca^{2+}]_o$. *A*, *I–V* relationship from a representative cell before (○) and after (●) bath application of 0·5 mM-$CdCl_2$. The currents were elicited using 200 ms depolarizing pulses from $V_h = -80$ mV to indicated test potentials. *B*, whole-cell currents from the same cell after leakage subtraction of the cadmium-sensitive component. *C*, mean *I–V* relationship after leakage subtraction from sixteen cells (mean ± S.E.M.). Points without error bars, in this and all subsequent figures, indicate that the S.E.M. was less than the symbol size.

I–V was variable from cell to cell and ranged from −30 to −130 pA. The rate of decline of the current amplitude also varied from cell to cell ('run-down'). Only cells which exhibited a small amount (< 20%) of 'run-down' were used in this study. All subsequent figures and traces are shown after subtraction of the $CdCl_2$-insensitive current, unless otherwise indicated.

The selectivity of this inward current on external $[Ca^{2+}]$ was studied using three different Ca^{2+} concentrations ($[Ca^{2+}]_o$ = 2·2, 5·0 and 10·0 mM). The total divalent

cation concentration was kept constant at 11 mM to minimize changes in surface charge by adding the appropriate amounts of $MgCl_2$ to the external solution. Figure 3*A* shows an example of an *I–V* relationship of a cell at the three different Ca^{2+} concentrations. In these experiments ($n = 7$): (i) the threshold for activation

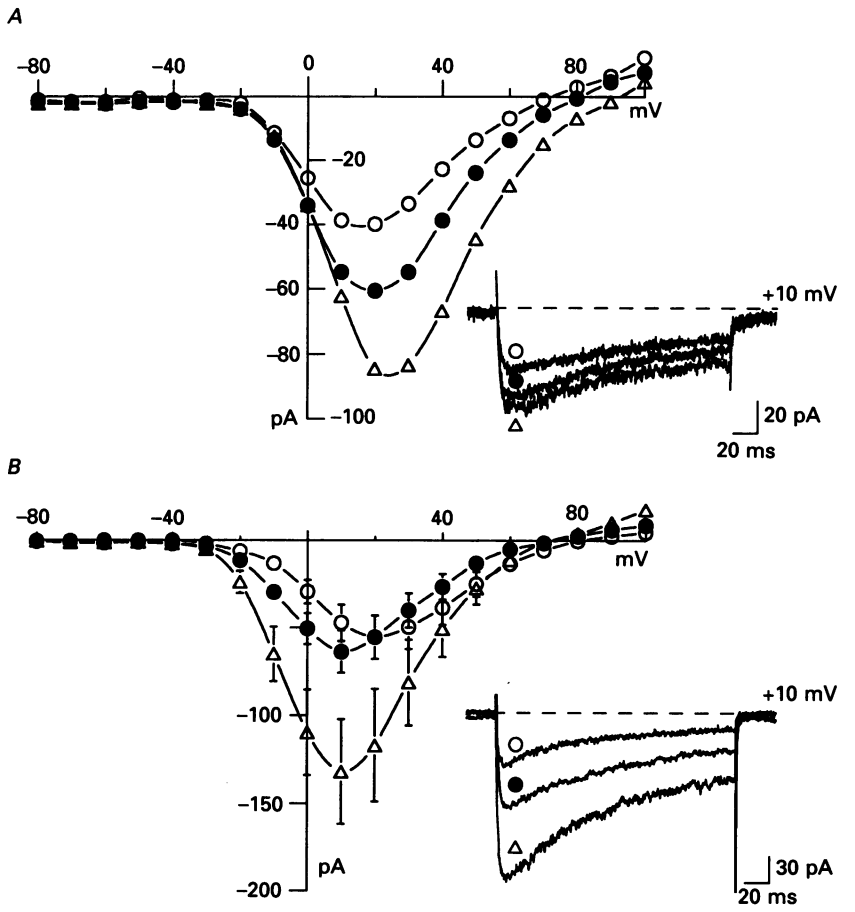

Fig. 3. The permeability and selectivity of I_{Ca} in coronary artery smooth muscle cells. *A*, *I–V* relationship and whole-cell currents (inset) from a representative cell after leakage subtraction showing the effect of changing $[Ca^{2+}]_o$ from 2·2 mM (○) to 5·0 mM (●) and 10·0 mM (△). Holding potential was −80 mV and the appropriate amount of $[Mg^{2+}]_o$ was changed to keep divalent ion concentration constant. *B*, *I–V* relationship (mean ± S.E.M., $n = 5$) showing the effect of changing the charge carrier from 10 mM $[Ca^{2+}]_o$ (○) to 10 mM $[Sr^{2+}]_o$ (●) and 10 mM $[Ba^{2+}]_o$ (△). The holding potential was −80 mV. The inset shows representative leak-subtracted whole-cell currents from a cell depolarized to 10 mV from $V_h = -80$ mV.

(−30 mV) did not change with increasing $[Ca^{2+}]_o$, (ii) the peak of the *I–V* was at approximately +20 mV, and (iii) the observed apparent reversal potential was shifted to more positive potentials. The inset of Fig. 3*A* shows three superimposed current records elicited at a test potential of +10 mV from a holding potential of −80 mV. The amplitudes of these three currents were 39·8, 59·1 and 85·2 pA for

$[Ca^{2+}]_o$ of 2·2, 5·0 and 10·0 mM respectively. The average time constants of inactivation at +10 mV in 10 mM $[Ca^{2+}]_o$ ($n = 8$) were significantly faster ($P < 0.05$) than those measured in 2·5 mM $[Ca^{2+}]_o$ ($n = 10$). The apparent reversal potentials (E_{rev}) averaged from seven separate experiments were $+69.5 \pm 1.4$, $+80.1 \pm 1.3$, and $+89.4 \pm 1.6$ mV (mean ± S.E.M.) for the three different calcium concentrations. The change in E_{rev} for a 10-fold change in $[Ca^{2+}]_o$ was calculated to be 33.0 ± 2.2 mV. This is close to the expected 30 mV shift in E_{rev} assuming a perfectly selective Ca^{2+} electrode.

The relative permeability changes to different divalent cations was tested sequentially using 10 mM solutions of Ca^{2+}, Sr^{2+} and Ba^{2+} as divalent charge carriers. The mean *I–V* constructed from five separate experiments is shown in Fig. 3*B* along with representative current traces from a cell showing the inward current elicited at a test potential to +10 mV from a holding potential of −80 mV in the three different divalent cation solutions. Magnesium was not added to any of the solutions. The activation threshold and apparent reversal potential were similar in all three solutions, but the peak of the *I–V* was shifted by 10 mV in the hyperpolarizing direction in both Sr^{2+} and Ba^{2+}. The averaged peak currents in five cells sequentially superfused with 10 mM-Ba^{2+}, 10 mM-Sr^{2+} and 10 mM-Ca^{2+} were -131 ± 30, -63 ± 12, and -55 ± 12 pA respectively. When the peaks of the *I–V* were normalized to the Ca^{2+} *I–V*, the order of relative permeability was $Ba^{2+}(2.38) > Sr^{2+}(1.15) > Ca^{2+}(1.00)$. The average time constants of inactivation for a test potential of +10 mV were 50.1 ± 3.9, 80.81 ± 13.5, and 87.8 ± 12.0 ms (mean ± S.E.M., $n = 4$) for Ca^{2+}, Sr^{2+} and Ba^{2+} respectively.

The effect of holding potential on I_{Ca} in normal-calcium and high-barium solutions

Several investigators have been able to separate two types of calcium currents (T-type and L-type) in vascular smooth muscle (Bean, 1989). When the low-threshold, rapidly inactivating T-type current is inactivated by using a depolarized holding potential, the L-type currents may be studied in isolation. At more hyperpolarized holding potentials, both types of currents are activated and the low-threshold T-type current is observed after the high-threshold L-type current is subtracted from the total current. In those studies, a holding potential of −30 mV was sufficient to completely inactivate T-type currents in 110 mM $[Ba^{2+}]_o$. Figure 4*A* shows the averaged *I–V* relationship from thirteen cells in 110 mM $[Ba^{2+}]_o$ using a holding potential of −80 mV (○) and −30 mV (●). At both potentials: (i) the threshold of activation was at −10 mV, (ii) the peak of the *I–V* was at +40 mV and (iii) the apparent reversal potential was at approximately +95 mV. The current amplitudes were not significantly altered when the holding potential was −30 mV. Digital subtraction of the −30 mV holding potential currents from the −80 mV holding potential currents did not reveal a rapidly inactivating component at any of the test potentials. Superimposed current traces from a cell in 110 mM $[Ba^{2+}]_o$ at the two different holding potentials are shown in Fig. 4*B*. The currents exhibited a much slower inactivation time course than the currents in 2·5 mM $[Ca^{2+}]_o$. In addition, depolarizing steps to 0 mV and +10 mV showed no rapidly inactivating component where the T-type current typically peaks in 110 mM $[Ba^{2+}]_o$ for other vascular smooth muscle cells (Bean, 1989).

We also attempted to isolate T-type currents by using two different holding

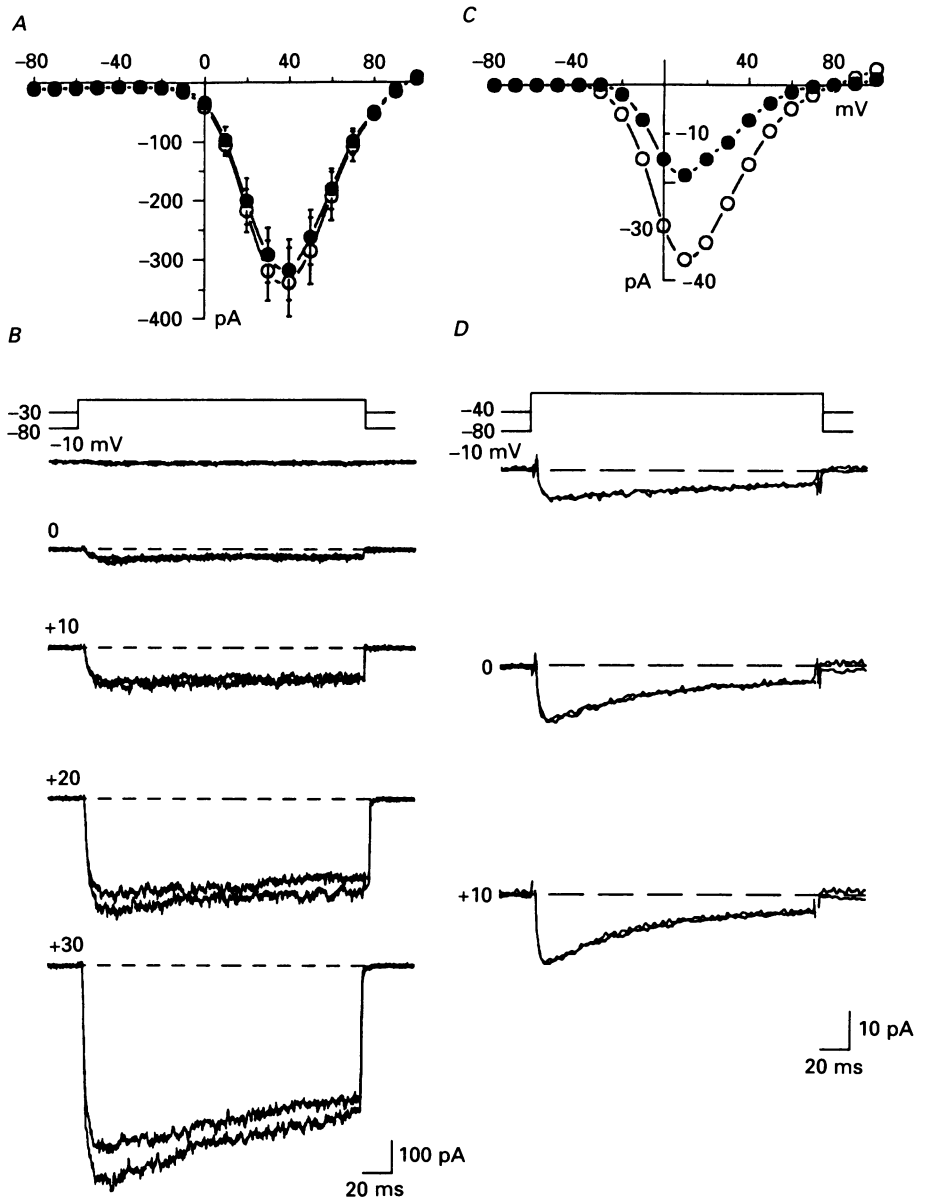

Fig. 4. Holding potential dependence of I_{Ca} using two different holding potentials in 110 mM $[Ba^{2+}]_o$ and in 2·5 mM $[Ca^{2+}]_o$. *A* shows the *I–V* relationship in 110 mM $[Ba^{2+}]_o$ at $V_h = -80$ mV (○) and $V_h = -30$ mV (●). Values are means ± S.E.M., $n = 13$, taken from non-leak-subtracted currents. *B*, superimposed leak-subtracted currents from a representative cell in 110 mM $[Ba^{2+}]_o$ at $V_h = -80$ mV and $V_h = -30$ mV using 200 ms depolarizing pulses to the indicated test potentials. *C*, *I–V* relationship from a cell in 2·5 mM $[Ca^{2+}]_o$ from $V_h = -80$ mV (○) and $V_h = -40$ mV (●) after leak subtraction. *D*, leak-subtracted currents from the same cell in *C* using 200 ms depolarizations to the indicated test potentials. The currents from $V_h = -40$ mV were scaled up by a factor of 2·0 and superimposed on currents to the same test potential from $V_h = -80$ mV. Traces in *D* were digitally filtered at 200 Hz which did not alter the decay kinetics.

potentials in 2·5 mM $[Ca^{2+}]_o$. Figure 4*C* shows a representative *I–V* from one cell using holding potentials of −80 mV (○) and −40 mV (●). The only apparent difference in the *I–V* characteristics appear to be a reduction in amplitude at a holding potential of −40 mV for all potentials in the activation range of I_{Ca}. The superimposed current

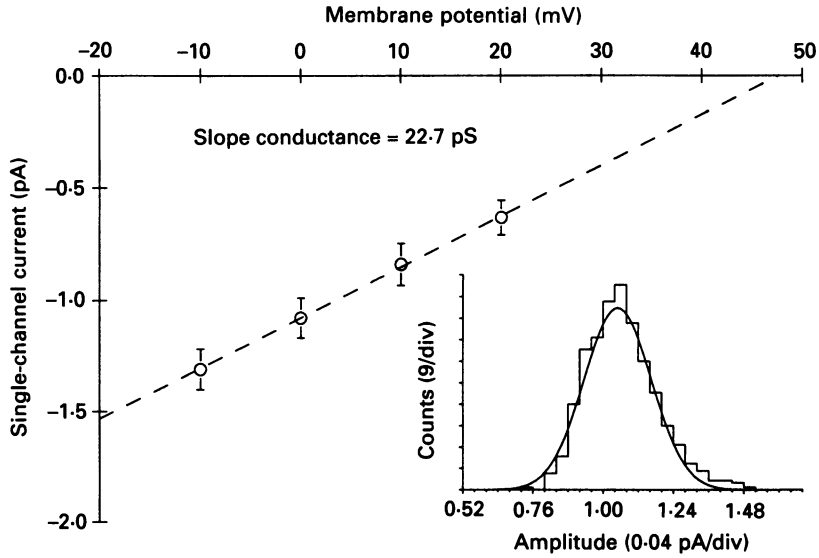

Fig. 5. The single-channel conductance of I_{Ca}. Unitary current amplitude is plotted *versus* membrane potential for a representative cell in the cell-attached configuration. The pipette solution contained 110 mM-$BaCl_2$ and the bath solution contained 140 mM-potassium to zero membrane potential. The patches were held at −80 mV and pulsed to the desired potential for 290 ms. Current amplitudes are mean ± S.D. taken from amplitude histograms of multiple traces at each potential. Inset: a representative amplitude histogram fitted with a single Gaussian function, for 588 events at a membrane potential of 0 mV.

tracings for the same cell at the indicated test potential are shown in Fig. 4*D*. After scaling the smaller current up by a factor of two, the currents are virtually superimposable suggesting that the difference in amplitude at the two holding potentials is due to inactivation, not separate current types.

In the single-channel experiments, approximately 67% of all patches that were sealed contained at least some calcium channel activity. Figure 5 shows a plot of unitary current amplitude *versus* membrane potential after a step from −80 mV from one cell. The best-fit line through these points has a slope of 22·7 pS which is within the expected range for an L-type calcium current. The mean slope conductance for nineteen cells was 20·7 ± 0·8 pS.

The effects of nickel and dihydropyridines on I_{Ca}

To further explore the presence of a T-type calcium channel in our preparation, the blocking effects of low concentrations of nickel ions (Ni^{2+}) were tested in both 2·5 mM $[Ca^{2+}]_o$ and 2·5 mM $[Ba^{2+}]_o$ solutions. From a holding potential of −80 mV, depolarizing voltage-clamp steps were applied from −70 to +70 mV in the absence

and presence of 40–100 μM-$NiCl_2$. In seven cells, there was no change in the current amplitude or the inactivation time course at any potential (data not shown).

The effect of the calcium channel agonist Bay K 8644 was studied in both calcium and barium solutions. Figure 6*A* shows a representative *I–V* and two superimposed

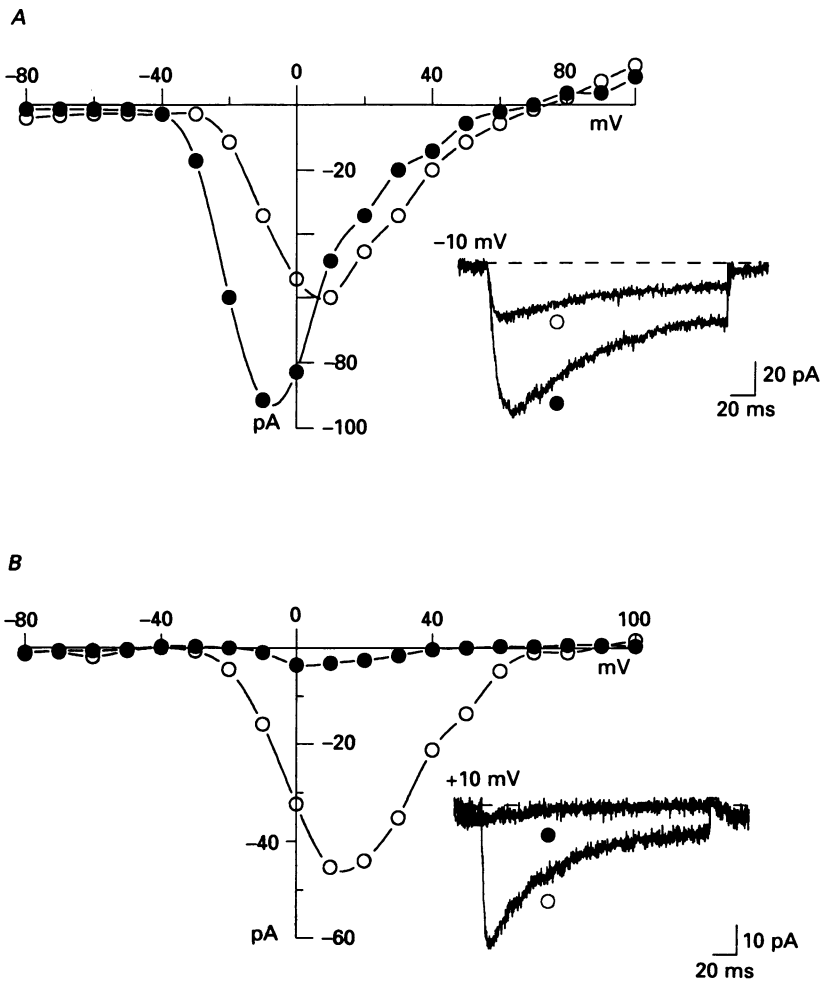

Fig. 6. The effect of the dihydropyridines Bay K 8644 and nifedipine on I_{Ca} in 2·5 mM $[Ca^{2+}]_o$. *A* shows the *I–V* relationship from a representative cell before (○) and approximately 5 min after bath application of 1 μM-Bay K 8644 (●). The inset shows two superimposed leak-subtracted current traces from the same cell at a test potential of −10 mV. *B*, shows the same experiment using 1 μM-nifedipine. The current traces in the inset were elicited using a test potential of +10 mV. The holding potential was −80 mV and the dashed lines represent zero current level in both panels.

current traces (inset) before (○) and after (●) bath application of 1 μM-Bay K 8644 in 2·5 mM $[Ca^{2+}]_o$. The peak amplitude increased from −61 to −91 pA in the presence of Bay K 8644. In addition, the peak of the Bay K 8644 *I–V* was shifted 20 mV in the hyperpolarizing direction. The effects of Bay K 8644 and nifedipine were fairly rapid, taking less than 3 min for maximal changes, but were difficult to

reverse without complications from run-down. When using 110 mM $[Ba^{2+}]_o$ as the charge carrier, the peak current amplitude increased from −550 pA in the control to −960 pA in 1 μM-Bay K 8644 with a 10 mV shift of the *I–V* peak in the hyperpolarizing direction (data not shown).

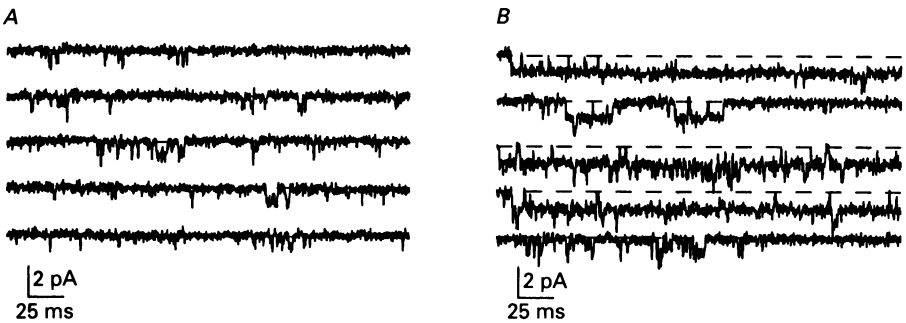

Fig. 7. The effect of Bay K 8644 on single calcium channel currents using 110 mM $[Ba^{2+}]_o$ as the charge carrier. *A* and *B* show five consecutive current traces elicited at a membrane potential of 0 mV from a holding potential of −80 mV. The beginning and end of the current traces represents the 'on' and 'off' of the voltage command pulse. Capacitative transients and leak currents were subtracted digitally using average current traces which contained no channel openings. The dashed lines represent the current level while the channels were closed. Channel openings are seen as downward deflections. *A* shows typical channel activity with single-channel pipette solution in the pipette, and *B* represents channel activity in the same membrane patch after 1 μM-Bay K 8644 had been introduced into the pipette.

Single-channel recordings in Fig. 7 show the effects of internal pipette perfusion of a single patch with 1 μM-Bay K 8644. Before application of this drug (Fig. 7*A*), the channel activity was characterized by very brief openings. This was typically the case in patches not exposed to Bay K 8644. After exposure to Bay K 8644 (Fig. 7*B*), channel openings were much longer in duration, often lasting the entire 290 ms depolarization as shown in the first trace of Fig. 7*B*. This patch had at least two channels present. The unitary current amplitudes were not significantly changed by Bay K 8644.

The effects of the calcium channel antagonist nifedipine on I_{Ca} were also studied in these cells. Figure 6*B* shows a representative *I–V* and current traces from one cell in 2·5 mM $[Ca^{2+}]_o$ before (○) and after (●) bath application of 1 μM-nifedipine. Nifedipine reduced or completely inhibited I_{Ca} at all test potentials. The same experiment was done in 110 mM $[Ba^{2+}]_o$ with similar results (data not shown). Additional studies of 1 μM-nifedipine on single calcium channel activity show that the large amount of channel 'chattering' activity observed in the control records was inhibited by exposure to 1 μM-nifedipine (data not shown).

Steady-state voltage dependence of I_{Ca} gating variables

A modified double-pulse protocol was used to measure the steady-state inactivation (f_∞) of I_{Ca} as a function of membrane potential (cf. Gillespie & Meves, 1980) to study functional role of I_{Ca}. Depolarizing and hyperpolarizing pre-pulse potentials ranging from −120 to +40 mV were applied for a duration of 2 s.

Following a 5 ms interpulse interval at a potential of −80 mV, the membrane was displaced to a test potential of +10 mV for 200 ms. Steady-state inactivation was measured as the ratio of I/I_{max}, where I_{max} is the maximum current amplitude elicited during the test pulse to +10 mV after the most hyperpolarizing pre-pulse to

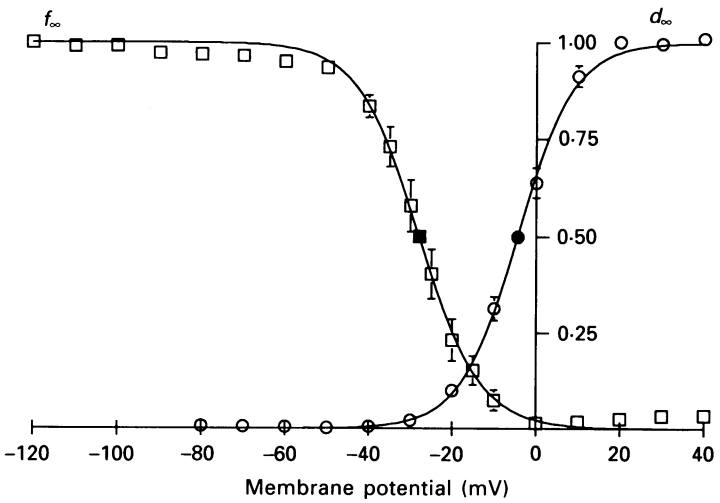

Fig. 8. Steady-state voltage dependence of the inactivation (f_∞) and activation (d_∞) of I_{Ca} in 2·5 mM $[Ca^{2+}]_o$. Inactivation data (□) are mean ± S.E.M. ($n = 6$) generated using a conventional paired-pulse protocol (see text). The points were fitted to a Boltzmann distribution equation, where $V_{\frac{1}{2}} = -27{\cdot}90 \pm 1{\cdot}8$ mV (■) and the slope factor $k = 6{\cdot}87 \pm 0{\cdot}36$. Activation data (○) are mean ± S.E.M. ($n = 16$) determined from the slope of the positive limb of the I–V relationship (see text). The d_∞ data points were also fitted to a Boltzmann distribution with $V_{\frac{1}{2}} = -4{\cdot}36 \pm 1{\cdot}14$ (●) and $k = -6{\cdot}29 \pm 0{\cdot}08$.

−120 mV. The −120 mV pre-pulse protocol followed each double-pulse protocol as its own control to account for 'run-down' of I_{Ca}. This current ratio was then plotted as a function of the pre-pulse potential. Figure 8 shows the average steady-state inactivation data (□) for I_{Ca} in 2·5 mM $[Ca^{2+}]_o$ ($n = 6$). The curve was well fitted by a conventional Boltzmann distribution of the following form:

$$f_\infty = \{1 + \exp[(V - V_{\frac{1}{2}})/k]\}^{-1}.$$

The half-inactivation potential ($V_{\frac{1}{2}}$) was $-27{\cdot}9 \pm 1{\cdot}8$ mV (■) with a slope factor (k) of $6{\cdot}9 \pm 0{\cdot}4$ mV (mean ± S.E.M.). Inactivation is nearly complete at approximately 0 mV and is fully removed at −100 mV. At pre-pulse potentials positive to +10 mV, the f_∞ curve showed a slight (5%) tendency for I_{Ca} during the test pulse to reactivate. Such a U-shaped inactivation curve has been interpreted to indicate evidence for a Ca^{2+}-dependent inactivation mechanism (Eckert & Tillotson, 1981; Klockner & Isenberg, 1985*c*). However, the major inactivation process appears to be strongly voltage dependent.

Characteristics of the steady-state activation variable (d_∞) were determined from the positive limb of the I–V relationship (Klockner & Isenberg, 1985*c*). The slope of the positive limb of the I–V was determined by a linear regression fit to the current amplitudes from +20 to +50 mV of each cell to obtain the maximum conductance

of I_{Ca}. The steady-state 'activation' curve was constructed using the following equation:

$$d_\infty = \text{peak}\, I_{Ca}/[g_{Ca}(V-E_{rev})],$$

where peak I_{Ca} is obtained from the I–V relationship and g_{Ca} is the maximal conductance value obtained from the linear regression line of the I–V extrapolated

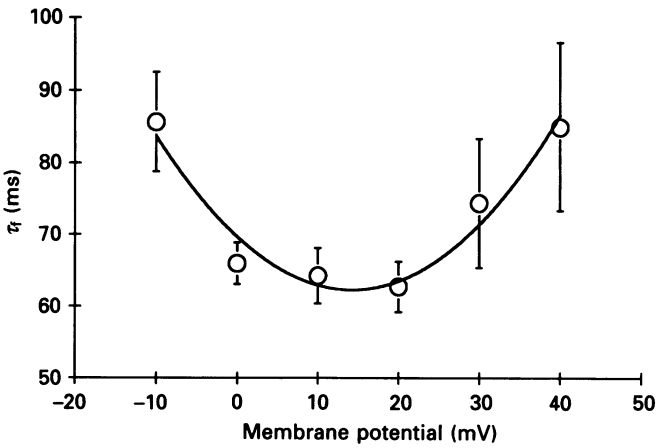

Fig. 9. The voltage dependence of the time constants of I_{Ca} inactivation (τ_f) in 2·5 mM $[Ca^{2+}]_o$. The data points represent mean ± S.E.M. (n = 10) as determined from DISCRETE analysis of 200 ms I_{Ca} current records. The data points were fitted by eye.

through the apparent reversal potential (E_{rev}). Figure 8 shows that the averaged activation curve (○) for I_{Ca} in 2·5 mM $[Ca^{2+}]_o$ is also shown to be well described by a Boltzmann distribution. The half-activation potential was −4·4 ± 1·1 mV (●) with a slope factor of −6·3 ± 0·1 mV (mean ± S.E.M., n = 16). These data show that the threshold for activation is at approximately −40 mV and is fully activated at approximately +20 mV.

Kinetic properties of I_{Ca} inactivation

The functional role of I_{Ca} was further investigated by characterizing the kinetic properties of the inactivation process. Figure 9 shows a plot of the time constant of inactivation (τ_f) *versus* membrane potential. In these experiments, the time course of I_{Ca} inactivation was best described by a single exponential function in approximately 80% of all the measurements. The remaining 20% of the measurements were best fitted by two exponentials but the single exponential fit also produced a reasonable fit when inspected visually. The single time constant values were averaged from ten cells in 2·5 mM $[Ca^{2+}]_o$. Step depolarizations from a holding potential of −80 mV to potentials ranging from −30 to +10 mV elicited an increase of I_{Ca} peak amplitudes. This was accompanied with a decrease in the time constant of inactivation. The fastest time constant of inactivation was observed at the peak of the I–V relationship, near +10 mV. Depolarizations greater than +20 mV elicited a decline of the peak calcium current amplitude with a concomitant decrease in the rate of inactivation up to +40 mV. We were not able to reliably fit the time course of activation for

potentials less than −10 mV or for potentials more positive than +40 mV due to the small size of the current. These results showed a U-shaped τ_f *versus* V_m relationship and is an indication for Ca^{2+}-dependent inactivation.

The rate of recovery from inactivation or reactivation was determined using a double-pulse protocol where identical 200 ms test pulses (P_I and P_{II}) to +10 mV

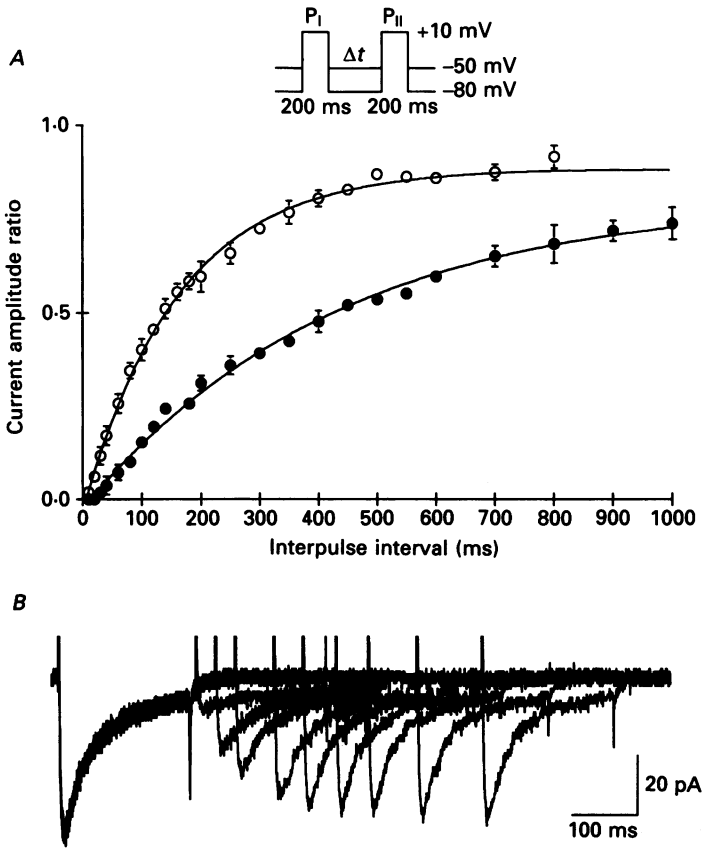

Fig. 10. Recovery from I_{Ca} inactivation in 2·5 mM $[Ca^{2+}]_o$. *A*, the voltage dependence of the time constant of recovery from inactivation using paired double-pulse protocols where $P_I = P_{II} = +10$ mV for 200 ms and Δt represents the increasing interpulse interval. Test pulses were applied from either $V_h = -80$ mV (○) or $V_h = -50$ mV (●). Values are mean ± S.E.M. $n = 5$. The data points were fitted by a single exponential with recovery time constants (τ) of 160·7 ms at $V_h = -80$ mV and 424·1 ms at $V_h = -50$ mV. *B*, representative currents elicited to a potential of +10 mV from a holding potential of −80 mV. The interpulse intervals used were 15, 40, 70, 120, 180, 220, 280, 350 and 450 ms.

were separated by increasing interpulse intervals (Δt) at two different holding potentials (−50 and −80 mV). The recovery curve was obtained by plotting the current amplitude ratio (P_{II}/P_I) as a function of the interpulse duration at each holding potential. Figure 10*A* shows average data from five different cells at interpulse potentials of −80 (○) and −50 mV (●). The time course of recovery from

inactivation was well described by a single-exponential process which showed marked voltage dependence. The recovery time constant (τ) of the averaged data was 160·7 ms at −80 mV and 424·1 ms at −50 mV, showing a 2·65-fold difference. Figure 10*B* shows representative current traces from one experiment at an interpulse

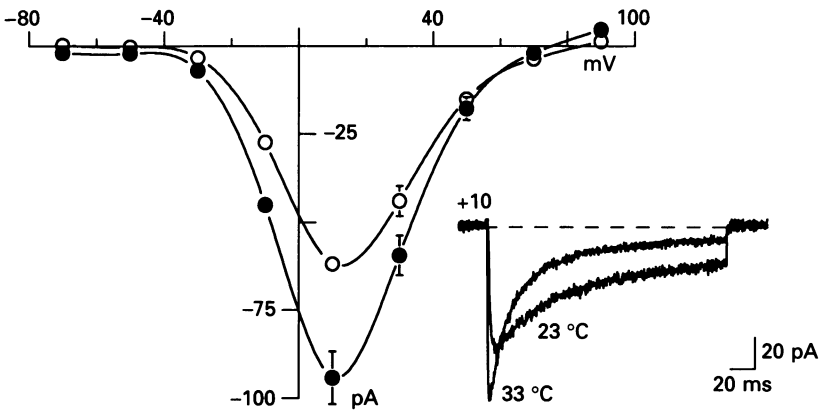

Fig. 11. The effects of temperature on I_{Ca} in 2·5 mM $[Ca^{2+}]_o$. The *I–V* relationship represents mean±S.E.M. ($n = 7$) at 23 °C (○) and 33 °C (●). The inset shows two superimposed leak-subtracted whole-cell currents elicited at a test potential of +10 mV from $V_h = -80$ mV at the two temperatures.

potential of −80 mV starting from an interpulse duration of 15 to 450 ms. The results from these experiments show that the recovery from inactivation of I_{Ca} was a potential-dependent process.

The effect of increasing temperature on I_{Ca}

Temperature-induced changes in I_{Ca} have not been studied in vascular smooth muscle. Figure 11 shows an average *I–V* for seven cells recorded at 23 °C (○) and 33 °C (●). The mean peak amplitudes were −59·9±3·2 pA at 23 °C, and −94·3±7·5 pA at 33 °C, resulting in a calculated Q_{10} of 1·57. In these experiments, the higher temperature was recorded after the lower temperature (approximately 3–4 min later) during which time run-down often took place. The range of Q_{10} values were from 1·28 to 2·31 but we believe the higher value is closer to the true Q_{10} due to complications with run-down at the higher temperature. Ganitkevich *et al.* (1987) obtained a similar Q_{10} value of 1·7±0·1 for peak I_{Ca} with a concurrent increase of inactivation kinetics in guinea-pig intestinal smooth muscle cells.

The inset of Figure 11 shows two superimposed current traces elicited from a holding potential of −80 mV to a depolarized potential of +10 mV at two temperatures. These current traces show that the rate of inactivation also increased at the higher temperature. Kinetic analysis revealed that at 33 °C I_{Ca} inactivation was best described by two time constants ($\tau_1 = 36·4±3·2$ ms, $\tau_2 = 9·5±2·1$ ms, $n = 6$ cells), while at 23 °C inactivation was best described by one time constant ($\tau = 51·9±5·0$ ms, $n = 7$ cells).

The effect of acetylcholine on I_{Ca}

Coronary arteries are innervated by both the sympathetic and parasympathetic nervous system (Gerova, 1982). We therefore studied the effects of the muscarinic agonist acetylcholine on I_{Ca}. Figure 12 shows a representative *I–V* and current traces

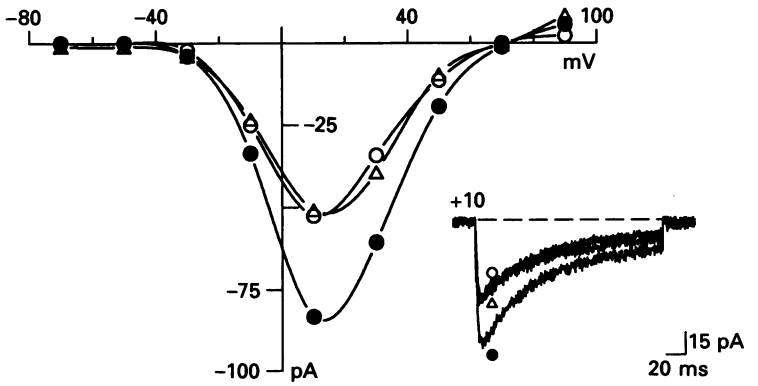

Fig. 12. The effect of acetylcholine on I_{Ca} in 2·5 mM $[Ca^{2+}]_o$. The *I–V* relationship from a representative cells is shown before (○) and after (●) bath application of 0·2 μM-ACh. Subsequent application of 1 μM-atropine in the presence of 0·2 μM-ACh (△) reversed the ACh effect to near control values. The inset shows three superimposed leak-subtracted whole-cell currents from the same cell at a test potential of +10 mV ($V_h = -80$ mV).

from one cell before (○) and after (●) bath application of 0·2 μM-ACh. The peak amplitude increased from −51 to −78 pA and was inhibited back to control levels with the application of 1 μM-atropine (△). A reversible increase in I_{Ca} was seen in eight out of thirteen cells. The average percentage increase in peak I_{Ca} was 39·5 ± 6·1 (mean ± S.E.M.) in the eight cells that showed an increase. The effects of ACh typically took greater than 4 min to occur and the increases in I_{Ca} were sustained for 6–10 min before washing in atropine.

DISCUSSION

Resting membrane potentials obtained from vascular smooth muscle tissue range from −25 to −65 mV and exhibit marked variations between vascular beds and species (Horn, 1978). In coronary arteries, resting potentials of −56 mV in the dog (Harder *et al.* 1979; Feletou & Vanhoutte, 1988) and −40·4 ± 4·9 mV in dispersed porcine cells (Sumimoto, Hirata & Kuriyama, 1988) have been measured. Our observation of −32 ± 10 mV may reflect the lack of an inwardly rectifying potassium current which is the major determinant of the negative resting potential in cardiac cells (Giles, van Ginneken & Shibata, 1986).

In twenty-two cells, the average cell capacitance was 18·5 ± 1·7 pF. This value is similar to that measured in canine saphenous vein (20 ± 5 pF, Yatani *et al.* 1987) and rat mesenteric artery (17·8 ± 1·5 pF, Bean, Sturek, Puga & Hermsmeyer, 1986) but smaller than the cell capacitance of rabbit ear artery (39 pF, Aaronson *et al.* 1988; 49 pF, Benham *et al.* 1987). A possible explanation for these differences could be due to differences in cell size from one circulation to another.

The existence of two types of voltage-dependent calcium currents has been described in a wide variety of vascular smooth muscle cells (for reviews see Aaronson *et al.* 1988; Bean, 1989). These currents are distinguishable by their differences in activation threshold, inactivation potential dependence, kinetics of inactivation, single-channel conductance and pharmacological sensitivities. In contrast to these vascular smooth muscle cells, our data in coronary artery smooth muscle show that there is only one type of calcium current which has characteristics of the L-type calcium current. Recently, however, Aaronson *et al.* (1988) showed that in the rabbit ear artery, separation of calcium currents into T- and L-type groups is an oversimplification and that the characteristics of the calcium currents which they describe show a continuum between the two groups.

The separation of vascular smooth muscle T- and L-type calcium currents can be achieved by eliciting test pulses from two different holding potentials (Benham *et al.* 1987). The subtracted current traces from two different holding potentials (-80 *versus* -40 mV in 2·5 mM $[Ca^{2+}]_o$ and -80 *versus* -30 mV in 110 mM $[Ba^{2+}]_o$) did not reveal a fast transient component indicative of a T-type calcium current. Furthermore, in both Ca^{2+} and Ba^{2+} solutions, the *I–V* relationship does not exhibit a 'bump' along the negative slope region due to the sum of two current components.

The T-type current has also been shown to have approximately equal permeability to both Ca^{2+} and Ba^{2+} whereas the L-type current is more permeable to Ba^{2+} than Ca^{2+} (Bean, 1989). In 10 mM $[Ca^{2+}]_o$ and $[Ba^{2+}]_o$ (Fig. 3*B*), Ba^{2+} was about 2–3 times more permeable than Ca^{2+}.

The sensitivity of L-type calcium currents and the relative insensitivity of T-type calcium currents to dihydropyridine Ca^{2+} agonists and antagonists has been well described (Bean, 1989). Consistent with these previous works in smooth muscle cells and in cardiac muscle (Sanguinetti, Krafte & Kass, 1986), the dihydropyridine agonist Bay K 8644 increases I_{Ca} and shifts the peak *I–V* relationship to more hyperpolarized potentials in both Ca^{2+} (Fig. 6) and Ba^{2+}. Our single-channel data (Fig. 7) also showed that Bay K 8644 prolongs the average channel-open time but does not significantly increase the single-channel current amplitude. Similar results were seen in other smooth muscle cells (Yatani *et al.* 1987). Nifedipine, a calcium channel blocker, inhibits peak I_{Ca} amplitude (Fig. 6) and single-channel openings. The degree of block is notably greater than that seen in single rabbit ear artery cells (Hering, Beech, Bolton & Lim, 1988) where 3 μM-nifedipine produced a 50% reduction in current. Herring *et al.* (1988) also observed that nifedipine induces a marked acceleration of the current decay. Interestingly, comparison of the control and scaled residual current after nifedipine blockade in our cells (Fig. 6) did not reveal any significant differences in the time course of current decay. We consider this as further evidence against the existence of a nifedipine-insensitive T-type calcium current.

Low concentrations of Ni^{2+} ions have been shown to preferentially inhibit T-type calcium currents (Bean, 1989). In the voltage range from -30 to 0 mV where the transient T-type current is least contaminated by L-type calcium currents, application of 40–100 μM-$NiCl_2$ in our rabbit coronary artery smooth muscle cells ($n = 7$) did not reveal a Ni^{2+}-sensitive component.

It is possible that the enzymatic dispersion procedure could have altered or

eliminated the low-threshold, dihydropyridine-insensitive, Ni^{2+}-sensitive, transient T-type calcium channel. We have tried combinations of shorter digestion times, lower enzyme concentrations, various enzyme vendors, and different trypsin and protease inhibitors with no difference in our results.

To determine the functional role of I_{Ca} in coronary smooth muscle cells it was essential to investigate the mechanism by which the calcium current inactivated. In vascular smooth muscle cells little is known about the inactivation process of the calcium current. Most studies have analysed the I_{Ca} decay as a purely voltage-dependent mechanism (Klockner & Isenberg, 1985*a*, *c*; Yatani *et al.* 1987). However, in recent studies, calcium currents from rabbit portal vein smooth muscle cells (Ohya, Kitamura & Kuriyama, 1988) and guinea-pig taenia caeci (Ganitkevich *et al.* 1986, 1987) were shown to have a marked U-shaped steady-state inactivation curve and the amplitude of I_{Ca} was dependent upon the intracellular concentrations of calcium ions. It was concluded that a major component of the inactivation process was Ca^{2+} dependent.

A Ca^{2+}-dependent inactivation mechanism would predict that the degree and rate of inactivation should be dependent upon the size of I_{Ca} (for review see Eckert & Chad, 1984). The steady-state inactivation curve (Fig. 8) suggests that at potentials more positive to the peak of the I_{Ca} *I–V* relationship where the amplitude of I_{Ca} is declining, there is a decrease in the degree of inactivation to approximately 0·05 at +40 mV. The time constant of inactivation *versus* potential curve in Fig. 9 shows that inactivation is fastest at the peak of the I_{Ca} *I–V* relationship and that inactivation is slowed when the current is made smaller. Increasing $[Ca^{2+}]_o$ also increased the rate of inactivation at a given potential. The kinetics of inactivation should also be dependent upon the species of the divalent cation. In the experiments shown in Fig. 3*B*, when 10 mM $[Ca^{2+}]_o$ was replaced with equimolar Ba^{2+} and Sr^{2+}, the time constants of inactivation for the Ba^{2+} and Sr^{2+} currents were slower than that of the Ca^{2+} current. However, it should be noted that Ba^{2+} and Sr^{2+} flowing through the calcium channel did not completely prevent inactivation of the current. Kass & Sanguinetti (1984) reported similar observations in cardiac calf Purkinje fibres and interpreted their results to show that the rates of inactivation of the Ba^{2+} and Sr^{2+} currents reflected the inherent kinetics of the voltage-dependent component of inactivation in the absence of the Ca^{2+}-dependent component. Although our data suggest a current-dependent component of inactivation, there is also strong evidence for a voltage-dependent process of inactivation. As indicated by the steady-state inactivation curve in Fig. 8, there is a substantial amount of inactivation at potentials before the current is activated and at potentials where the amplitude of I_{Ca} is very small. In addition, the rate of recovery of I_{Ca} exhibits a strong dependence upon membrane potential and does not appear to have a simple dependence to the amount of influx of calcium. In total, the data show that the inactivation mechanism of I_{Ca} in rabbit coronary artery smooth muscle cells is not a purely voltage-dependent process and that there is a current-dependent component involved in the inactivation process.

Since coronary arteries receive direct parasympathetic innervation (Gerova, 1982), and since muscarinic receptors (both M_1 and M_2) have been identified in coronary smooth muscle cells (Yamada, Yamazawa, Harada, Yamamura & Nakayama, 1988),

we attempted to determine the effect of acetylcholine on isolated rabbit coronary artery smooth muscle cells. An average percentage increase in I_{Ca} of $39{\cdot}5 \pm 6{\cdot}12$ ($n = 8$) was observed following bath application of 0·2 μM-acetylcholine. The enhanced ACh effect on I_{Ca} was inhibited by 1 μM-atropine. A similar ACh-induced I_{Ca} increase was observed in toad stomach smooth muscle cells (Clapp, Vivaudou, Walsh & Singer, 1987).

The number of Ca^{2+} channels in rabbit coronary artery smooth muscle cells can be estimated by the expression: $I = NiP$, where N is the number of channels in the membrane, i is the single-channel current and P is the probability of an individual channel being open (Tsien, 1983). The average peak current (I) at a test potential of +20 mV is approximately 217 pA in 110 mM $[Ba^{2+}]_o$. The probability of opening (P) was 0·13 and the single-channel conductance (i) was 0·53 pA averaged from four different cells at +20 mV. From the average cell surface area of $1{\cdot}87 \times 10^3$ μm^2, an estimate of channel density of 1·71 channels/μm^2 is obtained. This estimate of Ca^{2+} channel density is in good agreement with electrophysiological determinations from other cell types (Tsien, 1983).

This work was supported by grants from the National Institutes of Health (HL 41031 and HL 14388) to E. F. Shibata. We would like to thank Mr Jerry Jefson for his superb technical help.

REFERENCES

Aaronson, P. I., Bolton, T. B., Lang, R. J. & MacKenzie, I. (1988). Calcium currents in single isolated smooth muscle cells from the rabbit ear artery in normal-calcium and high-barium solutions. *Journal of Physiology* **405**, 57–75.

Bean, B. P. (1989). Classes of calcium channels in vertebrate cells. *Annual Review of Physiology* **51**, 367–384.

Bean, B. P., Sturek, M., Puga, A. & Hermsmeyer, K. (1986). Calcium channels in muscle cells isolated from rat mesenteric arteries: modulation by dihydropyridine drugs. *Circulation Research* **59**, 229–235.

Benham, C. D., Hess, P. & Tsien, R. W. (1987). Two types of calcium channels in single smooth muscle cells from rabbit ear artery studied with whole-cell and single-channel recordings. *Circulation Research* **61**, suppl. 1, 10–16.

Benham, C. D. & Tsien, R. W. (1988). Noradrenaline modulation of calcium channels in single smooth muscle cells from rabbit ear artery. *Journal of Physiology* **404**, 767–784.

Bolton, T. B., Lang, R. J., Takewaki, T. & Benham, C. D. (1985). Patch and whole-cell voltage clamp of single mammalian visceral and vascular smooth muscle cells. *Experientia* **41**, 887–894.

Chilean, W. M., Eastham, C. L. & Marcus, M. L. (1986). Microvascular distribution of coronary vascular resistance in the beating left ventricle. *American Journal of Physiology* **251**, H779–789.

Clapp, L. H., Vivaudou, M. B., Walsh, J. V. & Singer, J. J. (1987). Acetylcholine increases voltage-activated Ca^{2+} current in freshly dissociated smooth muscle cells. *Proceedings of the National Academy of Sciences of the USA* **84**, 2092–2096.

De La Lande, I. S., Harvey, J. A. & Holt, S. (1974). Response of rabbit coronary artery to autonomic agents. *Blood Vessels* **11**, 319–337.

Droogmans, G., Declerck, I. & Casteels, R. (1987). Effect of adrenergic agonists on Ca^{2+} channel currents in single vascular smooth muscle cells. *Pflügers Archiv* **409**, 7–12.

Eckert, R. & Tillotson, D. L. (1981). Calcium-mediated inactivation of the calcium conductance in caesium-loaded giant neurones of *Aplysia californica*. *Journal of Physiology* **314**, 265–280.

Eckert, R. & Chad, J. E. (1984). Inactivation of Ca channels. *Progress in Biophysics and Molecular Biology* **44**, 215–267.

Feigl, E. O. (1983). Coronary physiology. *Physiological Reviews* **63**, 1–205.

FELETOU, M. & VANHOUTTE, P. M. (1988). Endothelium-dependent hyperpolarization of canine coronary smooth muscle. *British Journal of Pharmacology* **93**, 515–524.

GANITKEVICH, V. YA., SHUBA, M. F. & SMIRNOV, S. V. (1986). Potential-dependent calcium inward current in a single isolated smooth muscle cell of the guinea-pig taenia caeci. *Journal of Physiology* **380**, 1–16.

GANITKEVICH, V. YA., SHUBA, M. F. & SMIRNOV, S. V. (1987). Calcium-dependent inactivation of potential-dependent calcium inward current in an isolated guinea-pig smooth muscle cell. *Journal of Physiology* **392**, 431–449.

GEROVA, M. (1982). Autonomic innervation of the coronary vasculature. In *The Coronary Artery*, ed. KALSNER, S., pp. 189–215. Croom Helm Ltd, London.

GILES, W., VAN GINNEKEN, A. & SHIBATA, E. F. (1986). Ionic currents underlying cardiac pacemaker activity: a summary of voltage clamp data from single cells. In *Cardiac Muscle: Regulation of Excitation and Contraction*, ed. NATHAN, R. D. Academic Press, Orlando, FL, USA.

GILLESPIE, W. F. & MEVES, H. (1980). The time course of sodium inactivation in squid giant axons. *Journal of Physiology* **299**, 289–307.

HAMILL, O. P., MARTY, A., NEHER, E., SAKMANN, B. & SIGWORTH, F. J. (1981). Improved patch-clamp techniques for high-resolution current recording from cells and cell-free membrane patches. *Pflügers Archiv* **391**, 85–100.

HARDER, D. R., BELARDINELLI, L., SPERELAKIS, N., RUBIO, R. & BERNE, R. M. (1979). Differential effects of adenosine and nitroglycerin on the action potentials of large and small coronary arteries. *Circulation Research* **44**, 176–182.

HERING, S., BEECH, D. J., BOLTON, T. B. & LIM, S. P. (1988). Action of nifedipine and Bay K 8644 is dependent on calcium channel state in single smooth muscle cells from rabbit ear artery. *Pflügers Archiv* **411**, 590–592.

HIRST, G. D. S., SILVERBERG, G. D. & VAN HELDEN, D. F. (1986). The action potential and underlying ionic currents in proximal rat middle cerebral arterioles. *Journal of Physiology* **371**, 289–304.

HORN, L. (1978). Electrophysiology of vascular smooth muscle. In *Microcirculation*, vol. 2, ed. KALEY, G. & ALTURA, B. M. University Park Press, Baltimore, MD, USA.

HUME, J. R. & GILES, W. (1981). Active and passive electrical properties of single bullfrog atrial cells. *Journal of General Physiology* **78**, 19–42.

JACK, J. J. B., NOBLE, D. & TSIEN, R. W. (1975). *Electrical Current Flow in Excitable Cells*. Clarendon Press, Oxford.

JOHNSON, E. A. & LIEBERMAN, M. (1971). Heart: excitation and contraction. *Annual Review of Physiology* **33**, 479–532.

KALSNER, S. (1989). Cholinergic constriction in the general circulation and its role in coronary artery spasm. *Circulation Research* **65**, 237–257.

KASS, R. S. & SANGUINETTI, M. C. (1984). Inactivation of calcium channel current in the calf cardiac Purkinje fiber. Evidence for voltage- and calcium-mediated mechanisms. *Journal of General Physiology* **84**, 705–726.

KLOCKNER, U. & ISENBERG, G. (1985*a*). Whole cell calcium channel currents (I_{Ca}) of smooth muscle cells isolated from bovine coronary arteries: effects of nifedipine and bay K 8644. *Pflügers Archiv* **403**, R22.

KLOCKNER, U. & ISENBERG, G. (1985*b*). Elementary currents through single Ca channels in smooth muscle cells isolated from bovine coronary arteries: effects of nifedipine and bay K 8644. *Pflügers Archiv* **403**, R23.

KLOCKNER, Y. & ISENBERG, G. (1985*c*). Calcium currents of caesium loaded isolated smooth muscle cells (urinary bladder of the guinea-pig). *Pflügers Archiv* **405**, 340–348.

MARTY, A. & NEHER, E. (1983). Tight-seal whole-cell recording. In *Single-Channel Recording*, ed. SAKMANN, B. & NEHER, E., pp. 107–121. Plenum Press, NY, USA.

MEKATA, F. (1980). Electrophysiological studies of the smooth muscle cell membrane of the dog coronary artery. *Journal of Physiology* **298**, 205–212.

NEHER, E. & ECKERT, R. (1987). Fast patch-pipette internal perfusion with minimum solution flow. In *Calcium and Ion Channel Modulation*, ed. GRINNELL, A. D., ARMSTRONG, D. A. & JACKSON, M. B., pp. 371–377. Plenum Press, NY, USA.

NELSON, M. T., STANDEN, N. B., BRAYDEN, J. E. & WORLEY, J. E. III (1988). Noradrenaline contracts arteries by activating voltage-dependent calcium channels. *Nature* **336**, 382–385.

OHYA, Y., KITAMURA, K. & KURIYAMA, H. (1988). Regulation of calcium current by intracellular calcium in smooth muscle cells of rabbit portal vein. *Circulation Research* **62**, 375–383.

PROVENCHER, S. W. (1976). A Fourier method for analysis of exponential decay curves. *Biophysical Journal* **16**, 27–41.

SANGUINETTI, M. C., KRAFTE, D. S. & KASS, R. S. (1986). Voltage-dependent modulation of Ca channel current in heart cells by Bay K8644. *Journal of General Physiology* **88**, 369–392.

SHEPHERD, J. T. & VANHOUTTE, P. M. (1986). Mechanisms responsible for coronary vasospasm. *Journal of the American College of Cardiology* **8**, 50–54 A.

SUMIMOTO, K., HIRATA, M. & KURIYAMA, H. (1988). Characterization of [^{3}H]nifedipine binding to intact vascular smooth muscle cells. *American Journal of Physiology* **254**, C45–52.

TSIEN, R. W. (1983). Calcium currents in excitable cell membranes. *Annual Review of Physiology* **45**, 341–358.

WEIDMANN, S. (1952). The electrical constants of Purkinje fibres. *Journal of Physiology* **118**, 348–360.

YAMADA, S., YAMAZAWA, T., HARADA, Y., YAMAMURA, H. I. & NAKAYAMA, K. (1988). Muscarinic receptor subtype in porcine coronary artery. *European Journal of Pharmacology* **150**, 373–376.

YATANI, A., SEIDEL, C. L., ALLEN, J. & BROWN, A M. (1987). Whole-cell and single-channel calcium currents of isolated smooth muscle cells from saphenous vein. *Circulation Research* **60**, 523–533.